Clim. Past Discuss., doi:10.5194/cp-2015-182, 2016
Manuscript under review for journal Clim. Past
Published: 26 January 2016

Climate of the Past Discussions
Open Access
EGU

Orbital control on the timing of oceanic anoxia in the Late Cretaceous

S. J. Batenburg[1,2], D. De Vleeschouwer[3,4], M. Sprovieri[5], F. J. Hilgen[6], A. S. Gale[7], B. S. Singer[8], C. Koeberl[9,10], R. Coccioni[11], P. Claeys[4], A. Montanari[12]

[1] Department of Earth Sciences, University of Oxford, Oxford, United Kingdom
[2] Institut für Geowissenschaften, Goethe-Universität Frankfurt, Frankfurt am Main, Germany
[3] MARUM, Universität Bremen, 28359 Bremen, Germany
[4] Earth System Sciences, Vrije Universiteit Brussel, 1150 Brussels, Belgium
[5] IAMC-CNR Capo Granitola, Campobello di Mazara, Italy
[6] Department of Earth Sciences, Utrecht University, Utrecht, the Netherlands
[7] School of Earth and Environmental Sciences, University of Portsmouth, Portsmouth, United Kingdom
[8] Department of Geoscience, University of Wisconsin-Madison, Madison, Wisconsin, United States of America
[9] Department of Lithospheric Research, University of Vienna, Vienna, Austria
[10] Natural History Museum Vienna, Vienna, Austria
[11] Dipartimento di Scienze della Terra, della Vita e dell'Ambiente, Università degli Studi "Carlo Bo", Urbino, Italy
[12] Osservatorio Geologico di Coldigioco, 62020 Frontale di Apiro, Italy

Correspondence to: S. J. Batenburg (sbatenburg@gmail.com)

Abstract. The oceans at the time of the Cenomanian-Turonian transition were abruptly disturbed by a period of bottom-water anoxia. This led to the brief but widespread deposition of black organic-rich shales, such as the Livello Bonarelli in the Umbria-Marche Basin (Italy). Despite intense studies, the origin and exact timing of this event are still debated. In this study, we assess leading hypotheses about the inception of oceanic anoxia in the Late Cretaceous greenhouse world, by providing a 6-Myr-long astronomically-tuned timescale across the Cenomanian-Turonian boundary. We procure insights in the relationship between orbital forcing and the Late Cretaceous carbon cycle by deciphering the imprint of astronomical cycles on lithologic, geophysical, and stable isotope records, obtained from the Bottaccione, Contessa and Furlo sections in the Umbria-Marche Basin. The deposition of black shales and cherts, as well as the onset of oceanic anoxia, is related to maxima in the 405-kyr cycle of eccentricity-modulated precession. Correlation to radioisotopic ages from the Western Interior (USA) provides unprecedented age control for the studied Italian successions. The most likely tuned age for the Livello Bonarelli base is 94.17 ± 0.15 Ma (tuning #1); however a 405-kyr older age cannot be excluded (tuning #2) due to uncertainties in stratigraphic correlation, radioisotopic dating, and orbital configuration. Our preferred tuning #1 suggests that the exact timing of major carbon cycle perturbations during the Cretaceous may be linked to increased variability in seasonality (i.e. a 405-kyr eccentricity maximum) after the prolonged avoidance of seasonal extremes (i.e. a 2.4-Myr eccentricity minimum). Volcanism was probably the ultimate driver of oceanic anoxia, but the exact timing of carbon cycle perturbations in the Late Cretaceous was likely determined by orbital periodicities. This unites two leading hypotheses about the inception of oceanic anoxia in the Late Cretaceous greenhouse world.

Clim. Past Discuss., doi:10.5194/cp-2015-182, 2016
Manuscript under review for journal Clim. Past
Published: 26 January 2016

Climate of the Past Discussions
Open Access
EGU

1 Introduction

The organic rich Livello Bonarelli formed as a result of oxygen deficiency and carbonate dissolution in the oceans during the Cenomanian/Turonian (C/T) transition. During this Ocean Anoxic Event 2 (OAE2), a combination of factors caused increased productivity, incomplete decomposition of organic matter and widespread deposition of black shales. Although these sediments are extensively studied, the exact extent, cause, timing and duration of oceanic anoxia are debated (Sinton and Duncan, 1997; Mitchell et al., 2008). Contrasting causal mechanisms have been suggested, including stratification of the water column (Lanci et al., 2010) versus intensification of the hydrological cycle driving a dynamic ocean circulation (Trabucho-Alexandre et al., 2010). Studies on trace-elemental and (radiogenic) isotope compositions of Cenomanian marine successions have suggested a volcanic origin of OAE2, by delivering nutrients to the semi-enclosed proto-North Atlantic (Zheng et al., 2013, and references therein; Du Vivier et al., 2014). Deciphering the importance of volcanic and oceanographic processes requires tight constraints on their relative timing. Regularly occurring black cherts and shales below the Livello Bonarelli demonstrate that oceanic conditions in the Umbria-Marche Basin were punctuated by episodes of regional anoxia from the mid-Cenomanian onwards. Their hierarchical stacking pattern suggests an orbital control on the deposition of organic rich horizons (Mitchell et al., 2008; Lanci et al., 2010). Stable carbon isotope data reveal that long-term variations in eccentricity paced the carbon cycle (Sprovieri et al., 2013) and sea level changes (Voigt et al., 2006) of the Late Cretaceous. Here we investigate the role of orbital forcing on climate and the carbon cycle, and, specifically, on organic-rich sedimentation prior, during, and after OAE2.

We also explore the potential for establishing an anchored astrochronology for the C/T interval in Europe. Recent improvements in the astronomical solution (La2011; Laskar et al., 2011b) and in the intercalibration of radiometric and astronomical dating techniques (Kuiper et al., 2008; Renne et al., 2013) allow the extension of the astronomical time scale into the Cretaceous. The C/T boundary in the Western Interior (USA) has been dated at 93.90 ± 0.15 Ma by intercalibration of radio-isotopic and astrochronologic time scales (Meyers et al., 2012b). Also, reinterpretation of proxy records spanning the C/T interval seems to resolve discrepancies in reported durations of the OAE2 (Sageman et al., 2006; Meyers et al., 2012a). The well-documented Italian rhythmic successions, reference sections for climatic processes in the Tethyan realm, need to be tied in with the absolute time scale. Biostratigraphic correlation to radioisotopically-dated ash beds in the Western Interior is complicated by the provinciality of faunas and floras. However, $\delta^{13}C$ stratigraphy provides a reliable correlation tool (Gale et al., 2005) and we present a new $^{40}Ar/^{39}Ar$ age for the Thatcher bentonite from the Western Interior occurring within the mid-Cenomanian $\delta^{13}C$ event (MCE). This study integrates the well-developed cyclostratigraphy from the Umbria-Marche Basin with radioisotopic ages from the Western Interior and derives a numerical timescale for this critical interval in Earth's history.

Clim. Past Discuss., doi:10.5194/cp-2015-182, 2016
Manuscript under review for journal Clim. Past
Published: 26 January 2016

2 Materials and Methods

2.1 Geological setting and proxy records

In the Umbria-Marche Basin (Fig. 1), the Livello Bonarelli separates the Cenomanian white limestones of the Scaglia Bianca from the Turonian pink limestones of the Scaglia Rossa. In this study, we present new geophysical and stable isotope data that were generated from the Cenomanian interval at the Furlo quarry, and from uppermost Cenomanian and Turonian deposits in the Gola del Bottaccione. In addition, stable carbon and oxygen isotope data were used from the Turonian of the Contessa quarry, published by Stoll and Schrag (2000). The proxy records from the Bottaccione, Contessa and Furlo sections are all presented on the same height scale, using the recent height scale for the Cretaceous Umbria-Marche basin introduced by Sprovieri et al. (2013).

The W4 member of the Scaglia Bianca formation at Furlo (Coccioni, 1996) consists mainly of light grey to white pelagic biomicrite alternating with light grey nodular to bedded cherts and tabular black cherts (Mitchell et al., 2008). The section was logged in detail and sampled at 3 cm spacing with an electric handheld drill. The total light reflectance (L*, in %) was measured with a Konica Minolta Spectrophotometer CM 2002 on the surface of rock powders, recording the reflected energy (RSC) at 400 to 700 nm wavelengths in 10-nm steps (averaged over three measurements). From the Furlo section, $\delta^{18}O$ and $\delta^{13}C$ were measured with a GasBench II device and a ThermoElectron Delta Plus XP mass spectrometer at the IAMC-CNR in Naples.

The overlying Livello Bonarelli consists of alternating 5-50 mm layers of organic-rich black shale (up to 26% TOC) and lighter radiolarite (Kuroda et al., 2007). The Bonarelli interval was sampled at a 2 cm resolution at both the Furlo and Bottaccione sections. Contents of major and selected minor elements from the Livello Bonarelli were determined with a Philips PW2400 sequential X-ray fluorescence (XRF) spectrometer equipped with a Rh-excitation source at the University of Vienna. Loss on ignition data reflect the weight of volatile substances lost upon heating and give a measure of the organic content. Details of the analytical procedures and accuracies are similar to those given in Reimold et al. (1994).

The overlying Turonian R1 member of the Scaglia Rossa formation consists of pink pelagic limestones and marly limestones with nodular to laminar red to gray cherts (Montanari et al., 1989). 38 m above the Livello Bonarelli at the Bottaccione section were logged in detail and the section was sampled at 5 cm spacing from 10 m to 30m above the Livello Bonarelli. Magnetic Susceptibility (MS) was measured with a Bartington MS2B Dual Frequency magnetometer at the Osservatorio Geologico de Coldigioco (averaged over three measurements). Stable isotope ratios were measured with a Kiel III device and a ThermoFinnigan delta +XL mass spectrometer at the Vrije Universiteit Brussel.

2.2 Ar/Ar dating

A new $^{40}Ar/^{39}Ar$ age was obtained for the mid-Cenomanian event in the $\delta^{13}C$ record. Sample 91-0-03 is the same material used by Obradovich (1993); it is from an ash bed in the *Conlinoceros gilberti* ammonite zone in the Western Interior (USA), commonly known as the Thatcher bentonite. Laser fusion $^{40}Ar/^{39}Ar$ analyses of single sanidine crystals were performed at

Clim. Past Discuss., doi:10.5194/cp-2015-182, 2016
Manuscript under review for journal Clim. Past
Published: 26 January 2016

the WiscAr laboratory, University of Wiscoinisn-Madison following methods detailed in Sageman et al. (2014). A total of 53 crystals were dated. Eleven crystals that yielded less than 98.5% radiogenic ^{40}Ar were excluded from the mean, as was one inherited crystal that gave an apparent age greater than 101 Ma. Ages are calculated relative to 28.201 ± 0.046 Ma Fish Canyon sanidines (Kuiper et al., 2008) using the ^{40}K decay constants of Min et al. (2000).

2.3 Time series analysis

Time series analysis was carried out using the MTM-method (Thomson, 1982) with LOWSPEC background estimation (Meyers, 2012), as implemented in the R package "astrochron". We used three 2-π prolate tapers and confidence levels were calculated with the LOWESS-based (Cleveland, 1979) procedure of Ruckstuhl et al. (2001). The Continuous Wavelet Transform is used to decompose the one-dimensional time-series into their two-dimensional time–frequency representation. Band-pass filters are applied with Analyseries (Paillard et al., 1996). Sedimentation rates within the Scaglia Rossa and Scaglia Bianca Formations are estimated with the Evolutionary Average Spectral Misfit (E-ASM) method (Meyers and Sageman, 2007), using all frequencies for which the MTM harmonic F-test reports a line component that exceeds 80% probability. For the Bonarelli level, sedimentation rate is estimated with the standard ASM method. Predicted orbital periods for the late Cretaceous (93 Ma) are from Berger et al. (1992).

3 Results

3.1 Lithology and proxy data

The Cenomanian black shales and cherts in the Furlo section display a hierarchical stacking pattern, with groups of 3 to 4 organic-rich levels, spaced ~20 cm apart (Figs. 2 & 3). The total reflectance record (L*, in %) captures this stacking pattern: grey and black cherts reflect little light and display shifts towards lower L* values, in contrast to the bright micritic Scaglia Bianca limestones with high L* values. Increased variability and negative values of $\delta^{13}C$ and $\delta^{18}O$ coincide with higher variability in reflectance and with the occurrence of organic rich layers.

XRF data from the Livello Bonarelli at Furlo display a marked variability at a 12-cm scale (Fig. 4). The TiO_2, and Al_2O_3 records display very similar behaviour, whereas SiO_2, and LOI data additionally show variation on a 40-cm scale. At Bottaccione, a marked variability can be observed at an 8-cm scale in the SiO_2, TiO_2 and Al_2O_3 data from the Livello Bonarelli (Fig. 5).

The Scaglia Rossa pelagic limestones were studied in the classic Contessa and Bottaccione sections near Gubbio. Oscillations between radiolarian cherts and foram-coccolith pelagic limestones show hierarchical bundles of 2 to 5 chert layers per bundle. These bundles could be correlated amongst the Contessa and Bottaccione sections and are indicated by circumflexes on Figure 3. The lithologic log shown on Figure 3 is for the Bottaccione section. The magnetic susceptibility signal of the Bottaccione section accentuates the hierarchical stacking pattern, showing an increased magnetic susceptibility signal in intervals characterized by frequent chert beds (Figure 3).

Clim. Past Discuss., doi:10.5194/cp-2015-182, 2016
Manuscript under review for journal Clim. Past
Published: 26 January 2016

Climate of the Past Discussions

3.2 Ar/Ar

The inverse variance weighted mean age of 41 of the 53 sanidine crystals measured from sample 91-0-03 give an age of 96.21 ± 0.16/0.36 Ma (2σ analytical uncertainty/full uncertainty including decay constant and standard age), with an MSWD of 0.69 (Figure 6). The complete set of analytical and standard data is in Suppl. Table 1.

3.3 Time series analysis

Spectral analyses by MTM/LOWSPEC, in combination with the evolutionary Average Spectral Misfit (ASM; Meyers and Sageman, 2007) method, suggest an average sedimentation rate around 11 m/Myr throughout the studied interval, excluding the Livello Bonarelli (Figs.7 & 8).

In the Cenomanian interval, the MTM/LOWSPEC spectra of all proxies exhibit a spectral peak exceeding the 95% CL for a cycle thickness of 0.25 m, corresponding to the spacing between individual chert layers, which is interpreted as the imprint of ~21-kyr precession (left column in Fig. 7). The average accumulation rate is 11 m/Myr (lower panel in Fig. 8) and the dominant periodicities at 1 and 4 m correspond to 100-kyr and 405-kyr eccentricity, respectively (Fig. 7).

Similarly, in the Turonian interval, a 0.25 m spectral peak exceeds the 95% CL for all proxies and is interpreted as the imprint of precession (right column in Fig. 7). Here, the eccentricity components are represented by dominant periodicities of 4.66 and 1.16 m and the average accumulation rate is 10.5 m/Myr (upper panel in Fig. 8).

We also find a statistically significant imprint of obliquity in Furlo's Cenomanian $\delta^{13}C$ record which confirms an important obliquity-control on the greenhouse carbon cycle, as suggested by Laurin et al. (2015). Grouping of precession-related chert-limestone alternations in ~100-kyr bundles is indicated by circumflexes next to the lithological log in Fig. 3 and 405-kyr eccentricity cycles are denoted by yellow-white alternating bands. The definition of eccentricity minima and maxima is based on the extremes of the 3-5 m bandpass filter of L* (Furlo), MS (Bottaccione), as well as and on the stacking pattern of shales and cherts (Bottaccione).

For the Livello Bonarelli from Furlo (124 cm), a duration estimate is obtained from 2-cm spaced X-Ray Fluorescence (XRF) spectrometry data. The multitaper method (MTM) spectral analyses of SiO_2 yield dominant periodicities of ~40, ~12, and ~6 cm (Fig. 3a). We calculate the ASM using the results of MTM harmonic analysis (>80%), and obtain an optimal sedimentation rate of 0.286 cm/kyr for the Bonarelli in Furlo. Hence, we interpret the reported periodicities as the imprint of short eccentricity, obliquity, and precession and estimate the duration of the Livello Bonarelli at 413 kyr.

ASM analysis of the Al_2O_3 data from the 82 cm thick Livello Bonarelli at Bottaccione suggests an optimal sedimentation rate of 0.208 cm/kyr (Fig. 5). ~8-cm thick cycles are interpreted as the imprint of obliquity, the duration of Livello Bonarelli at Bottaccione is estimated at 410 yr, comparable to the estimate of 413 kyr at Furlo.

Clim. Past Discuss., doi:10.5194/cp-2015-182, 2016
Manuscript under review for journal Clim. Past
Published: 26 January 2016

4 Discussion

4.1 Stable isotopes and diagenesis

The records of $\delta^{18}O$ and $\delta^{13}C$ show long-term trends over the successions, although the $\delta^{18}O$ record in particular displays scatter which might be due to an influence of diagenesis. $\delta^{13}C$ is generally more robust to post-depositional alteration (Jenkyns et al., 1994) and bulk carbonate $\delta^{13}C$ patterns have been shown to be a powerful tool for stratigraphic correlation, despite variations in absolute values and amplitude amongst locations (Jarvis et al., 2006). Although variability at the sampling scale (3 cm) may partially represent effects of diagenesis which could obscure short (precessional scale) climatic signals, the longer term trends compare well with coeval sections in the Umbria-Marche basin (Stoll and Schrag, 2000; Sprovieri et al., 2013) and the English chalk records (Jarvis et al., 2006) (Figure 9).

4.2 Astronomical forcing and phase relationships

Throughout the Cenomanian interval of the Furlo section, black cherts occur in distinct bands, which are often underlain by a thin layer of black shale. As these organic-rich horizons do not occur as nodules, they reflect a primary silica enrichment from radiolarian and/or diatom blooms. When present, black chert bands occur in groups with a regular spacing amongst them, likely reflecting a threshold response to extremes of the precessional cycle. Previous tuning attempts have placed black cherts either in eccentricity maxima (Voigt et al., 2006; Mitchell et al., 2008) or eccentricity minima (Lanci et al., 2010), entailing distinctly different oceanographic regimes. During eccentricity maxima, the seasonal contrast on the Northern Hemisphere is periodically enhanced during high-amplitude precession minima, thereby intensifying monsoons, leading to an estuarine circulation in the Cretaceous North Atlantic with upwelling and increased productivity (Mitchell et al., 2008), potentially spurred by input of nutrients from volcanic activity (Trabucho-Alexandre et al., 2010). Alternatively, it has been suggested that eccentricity minima could cause decreased seasonality, leading to stagnation and reduced ventilation of bottom waters (Lanci et al., 2010), although eccentricity minima would not lower seasonality but rather avoid large seasonal extremes for a prolonged period of time. This reverse phase relationship was deduced from the remanent magnetization within carbonates at Furlo (Lanci et al., 2010), incorrectly excluding cherts. The relationship between eccentricity forcing and ocean-climate response can be derived from the degree of variability in the presented data. Intervals marked by maximal lithological difference represent periods of large precessional amplitude during eccentricity maxima. Radiolarian cherts coincide with maximal amplitude of carbon and oxygen isotope signals and with a tendency of those proxies towards more negative values (Figures. 2 & 3). Negative $\delta^{18}O$ values may reflect warmer temperatures and a potentially increased influx of fresh water by increased monsoonal activity. Relatively low values of $\delta^{13}C$ could be associated with stratification of the water column and reduced yearly integrated primary productivity (Sprovieri et al., 2013). Conversely, high $\delta^{13}C$ values likely reflect good bottom water ventilation during eccentricity minima, with a prolonged avoidance of seasonal extremes, allowing for more stable primary productivity over the annual cycle which may have caused the increase in marine $\delta^{13}C$ (Figure 3). Possibly, the increased accumulation of organic carbon on land due to more uniform annual precipitation during eccentricity

Clim. Past Discuss., doi:10.5194/cp-2015-182, 2016
Manuscript under review for journal Clim. Past
Published: 26 January 2016

minima may have amplified the rise in marine $\delta^{13}C$, as suggested for Cenozoic intervals (Zachos et al., 2010). Figure 2 illustrates this phase relationship based on proxy records from the Cenomanian Furlo section. An analogous phase relationship for the proxy records from the Bottaccione sections was inferred. There, black cherts are absent from the Turonian interval of the succession, but grey cherts occur rhythmically throughout. Increased variability and negative values of $\delta^{13}C$ coincide with high variability in the magnetic susceptibility record in chert-rich intervals, associated with eccentricity maxima.

4.3 Anchoring the Astrochronology

4.3.1 Correlation of the C/T boundary

In this study, the base of the Turonian stage at Bottaccione is placed at 487.47 m, just above the first occurrence of *Quadrum gartneri* at 487.25 m defining the base of the C11 zone (Sissingh, 1977), following Sprovieri et al. (2013) and Tsikos et al. (2004). Direct comparison of high resolution $\delta^{13}C_{carb}$ data from Pueblo (Caron et al., 2006) with $\delta^{13}C_{carb}$ data from Contessa (Stoll and Schrag, 2001) allows for correlating $\delta^{13}C_{carb}$ maximum III in Pueblo with the $\delta^{13}C_{carb}$ maximum 85 cm above the Livello Bonarelli at 487.52 cm, comparable with its location at Bottaccione. An alternative correlation places the C/T boundary near a minimum in the $\delta^{13}C_{carb}$ data from the Gubbio S2 core (Trabucho-Alexandre et al., 2011) of Tsikos et al. (2004), which corresponds to the minimum in $\delta^{13}C_{carb}$ values at 488.22 m at Contessa (Stoll and Schrag, 2001), which is 75 cm above the C/T estimate adopted in this study. Consequently, 75 cm is taken as a conservative estimate of the stratigraphic uncertainty on the position of the C/T boundary, i.e. 487.47 ± 0.75 m. With an average sedimentation rate of 11 m/Myr, this stratigraphic error margin translates in a temporal uncertainty of ± 68 kyr.

4.3.2 Tuning options

Because of its stability, only the 405-kyr component of eccentricity can be used for astronomical tuning in the Cretaceous and not the ~100 kyr periodicity that was used in previous tuning efforts (Mitchell et al., 2008). The shorter obliquity and precession terms can only be used for the development of floating time scales. Two 405-kyr tuning options to astronomical solution La2011 remain if a C/T boundary age of 93.9 ± 0.15 Ma (Sageman et al., 2006; Meyers et al., 2012b) is considered, along stratigraphic uncertainty in the studied sections (± 0.068 Ma) and astronomical uncertainty. The uncertainty in the 405-kyr component of the astronomical target curve was estimated at ± 78.5 kyr, by determining the maximal difference between the position of minima in the 405-kyr band-pass filter outputs (300-625 kyr) of the La2010d, La2011 and La2011m2 solutions (Laskar et al., 2011a). The first 405-kyr minimum in the Turonian at 489.1 m in Bottaccione corresponds to the 405-kyr minimum in the astronomical solution at 93.5 ± 0.15 (tuning #1) or at 93.9 ± 0.15 Ma (tuning #2; Fig. 3).

Tuning options for the Cenomanian interval of this study depend on the duration of the Livello Bonarelli. The Livello Bonarelli in the Umbria-Marche basin reflects the culmination of OAE2, limited to the "2nd-build-up" and "plateau" of the OAE2 $\delta^{13}C$ excursion (Tsikos et al., 2004). The estimated duration in this study between the start of the $\delta^{13}C$ excursion,

Clim. Past Discuss., doi:10.5194/cp-2015-182, 2016
Manuscript under review for journal Clim. Past
Published: 26 January 2016

below the Livello Bonarelli, and the Cenomanian-Turonian boundary is ~490 kyr. This duration is slightly longer than a previous estimate from the German Wunstorf core of 430-445 kyr for the OAE2 isotope excursion (Voigt et al., 2008; Takashima et al., 2009), and slightly shorter than the duration of of 520 – 560 kyr from the "first build-up" to the "end of plateau", determined by intercalibration between radioisotopic and astrochronologic time-scales at the C/T GSSP (Sageman et al., 2006; Meyers et al., 2012b). Similar duration estimates for this interval were obtained by reinterpreting the orbital influence at Demerara Rise and Tarfaya (Meyers et al., 2012a), of 500-550 kyr and 450-500 kyr respectively, as well as in the Aristocrat-Angus-12-8 Core in Northern Colorado (Ma et al., 2014), of 516-613 kyr, albeit using a slightly different correlation.

The duration estimate for the Livello Bonarelli allows the extension of the astronomical tuning into the Cenomanian interval of this study. The base of the Livello Bonarelli corresponds to 94.19 Ma ± 0.15 (tuning #1) or 94.59 ± 0.15 Ma (tuning #2); i.e., the first short-eccentricity maximum after a 405-kyr minimum. Although seemingly similar to a previously reported (Mitchell et al., 2008) tuned age of 94.21 Ma, the latter would correspond to an age of 94.81 Ma after recalibration to revised standard ages (Kuiper et al., 2008).

4.3.3 Radioisotopic dating

Additional age control is provided by correlation of two Cenomanian ash beds from the Western Interior of the USA. Correlation to "Ash A" at the base of the boundary of the planktonic foraminifer biozones of *Whiteinella archaeocretacea* and *Rotalipora cushmani* (Leckie, 1985; Caron et al., 2006; Sageman et al., 2006) provides an independent age for this zonal boundary 7 cm below the base of the Bonarelli Level of 94.20 ± 0.28 Ma. This age is in closer agreement to tuning #1 (94.17 ± 0.15 Ma) than tuning #2 (94.57 ± 0.15 Ma), which can, however, not be excluded.

The MCE, characterized by a double positive peak in $\delta^{13}C$ at Furlo (first maximum at 466.47 m), offers another opportunity to test both tuning options. $^{40}Ar/^{39}Ar$ isotope data were acquired from 41 single sanidine crystals in sample 91-O-03 of Obradovich (1993) (methods outlined in Sageman et al., 2014), and yields an age of 96.21 ± 0.16/0.36 (2σ analytical and full uncertainty) for the Thatcher bentonite in the *Conlinceras tarrantense* zone at Pueblo, Colorado. This bentonite falls within the first peak of the MCE (Gale et al., 2008). In our tuning options, this level is either 96.09 ± 0.15 Ma (tuning #1) or 96.49 ± 0.15 Ma (tuning #2). Although tuning #1 is in close agreement with the new $^{40}Ar/^{39}Ar$ age, both tuning options remain possible. Nonetheless, the duration between radioisotopic age tie-points is consistent with cyclostratigraphy (Fig. 2) and provides tuned ages for biostratigraphic events (Table 1).

4.4 Long term behaviour of the carbon cycle

Although the occurrence of black layers increases up-section at Furlo, black cherts and shales are absent in the interval at 483-485 m, below the Livello Bonarelli. This may reflect the prolonged avoidance of seasonal extremes during long-term eccentricity minima. The first ~100-kyr bundle of black cherts following this interval contains exceptionally thick dark levels and corresponds to the beginning of the first 405-kyr maximum after the ~2.4-Myr minimum. Hence, we associate the onset

Clim. Past Discuss., doi:10.5194/cp-2015-182, 2016
Manuscript under review for journal Clim. Past
Published: 26 January 2016

of OAE2 with this 405-kyr maximum. Within the Livello Bonarelli, one can also visually observe the imprint of 100-kyr eccentricity cycles, comparable to the expression of OAE2 in the Sicilian Calabianca section (Scopelliti et al., 2006) and in the German Wunstorf core (Voigt et al., 2008). Ten obliquity cycles can be visually detected in the XRF-proxy data (Fig. 4b-e). Silica, delivered by radiolarian blooms, mirrors terrestrially derived components (Al_2O_3 and TiO_2) and may represent variations in seasonality and ventilation driven by obliquity during the deposition of the Livello Bonarelli.

Two pronounced 405 kyr minima, likely within a 2.4 Myr minimum, occur in the upper Cenomanian, the first of which could correspond (following tuning #1) to the interval lacking black shales at 483-485 m, and the second occurring within the Livello Bonarelli. The occurrence of two 405 kyr minima within a 2.4 Myr minimum could explain the observed presence of the ~100 kyr cyclicity within the Livello Bonarelli, as well as the influence of obliquity which was detected during OAE2 in several North Atlantic datasets (Meyers et al., 2012a). The Livello Bonarelli was previously suggested to coincide with a 2.4 Myr eccentricity minimum, invoking stagnation as forcing mechanism for anoxia (Mitchell et al., 2008). The relatively strong obliquity influence during the deposition of the Livello Bonarelli might be consistent with this orbital configuration (Hilgen et al., 2003).

The new astrochronologies allow for assessing the long-term behavior of the carbon cycle during the C/T transition. The onset of the MCE, the base of the Livello Bonarelli, and the middle of the negative $\delta^{13}C$ excursion of the mid-Turonian are separated by 2.0 Myr and 2.4 Myr, respectively. The 1.6 Myr long negative excursion in the mid-Turonian is characterized by an intermittent double positive peak ("Pewsey events"; Jarvis et al., 2006), similar to the MCE, starting at 91.7 Ma (tuning #1) or 92.1 Ma (tuning #2). These repetitive variations in $\delta^{13}C$, superimposed on the long-term behavior of the carbon cycle, are likely paced by the ~2.4-Myr eccentricity period. Following tuning #1, a tentative comparison with the full eccentricity solution La2011 (Fig. 2) reveals the occurrence of pronounced long-term minima in eccentricity before the mid-Cenomanian and mid-Turonian events.

Trace element studies indicate that volcanic activity of the Caribbean Large Igneous Province increasingly supplied nutrients and sulphate to a low-sulphate ocean, with a major pulse ~500 kyr before OAE2 (Snow et al., 2005; Jenkyns et al., 2007; Turgeon and Creaser, 2008; Adams et al., 2010). This is manifested by the increasing recurrence of black cherts through the Cenomanian interval, indicating that the western Tethys was progressively more prone to the development of anoxia due to a long-term trend of ongoing warming and increased volcanism. However, the exact timing of carbon cycle perturbations may be linked to a specific sequence of astronomical variations superimposed on this trend. The increased variability in seasonality, after the prolonged avoidance of seasonal extremes, was possibly responsible for observed intensification of the hydrological cycle, weathering, and more vigorous ocean circulation. Previously, Mitchell et al. (2008) placed OAE2 within the ~2.4 Myr minimum itself and suggested that the lack of strong insolation variability, associated with such a minimum, prevented the system from changing states and limestone deposition. However, our chronology advocates intensified circulation and upwelling, delivering nutrients from volcanism and weathering to the western Tethys and the North Atlantic, and triggering prolonged and widespread anoxia. In conclusion, the 6-Myr-long astronomically-tuned timescale across

Clim. Past Discuss., doi:10.5194/cp-2015-182, 2016
Manuscript under review for journal Clim. Past
Published: 26 January 2016

OAE2 presented in this study allows for the evaluation and combination of two leading hypotheses about OAE2 forcing mechanisms.

5 Acknowledgements

We would like to thank Stephen Meyers, Nicolas Thibault, Ian Jarvis, André Bornemann and an anonymous reviewer for comments on a previous version of the manuscript. DDV thanks the Research Foundation Flanders (FWO) for a Ph.D. scholarship and the EARTHSEQUENCING project (ERC Consolidator Grant). SJB thanks the European Community funded GTSnext project (grant agreement 215458), the European Science Foundation activity 'EARTHTIME—The European Contribution' (Exchange Grant 3818) and the German Research Foundation (DFG VO 687/14-1, IODP/ODP SSP 527/32).

6 References

Adams, D., Hurtgen, M., and Sageman, B.: Volcanic triggering of a biogeochemical cascade during Oceanic Anoxic Event 2, Nat. Geosci., 3, 201-204, doi:10.1038/ngeo743, 2010.

Berger, A., Loutre, M. F., and Laskar, J.: Stability of the Astronomical Frequencies Over the Earth's History for Paleoclimate Studies, 255, 560-566, 10.1126/science.255.5044.560, 1992.

Caron, M., Dall'Agnolo, S., Accarie, H., Barrera, E., Kauffman, E., Amédro, F., and Robaszynski, F.: High-resolution stratigraphy of the Cenomanian–Turonian boundary interval at Pueblo (USA) and wadi Bahloul (Tunisia): stable isotope and bio-events correlation, Geobios, 39, 171-200, doi:10.1016/j.geobios.2004.11.004, 2006.

Cleveland, W. S.: Robust Locally Weighted Regression and Smoothing Scatterplots, J. Amer. Statist. Assoc., 74, 829-836, doi:10.1080/01621459.1979.10481038, 1979.

Coccioni, R.: The Cretaceous of the Umbria-Marche Apennines (central Italy), Wiedmann Symposium bCretaceous Stratigraphy, Paleobiology and PaleobiogeographyQ, the Umbria–Marche Apennines (Central Italy). Tübingen, 1996, 7-10,

Du Vivier, A., Selby, D., Sageman, B., Jarvis, I., Gröcke, D., and Voigt, S.: Marine $^{187}Os/^{188}Os$ isotope stratigraphy reveals the interaction of volcanism and ocean circulation during Oceanic Anoxic Event 2, Earth Planet. Sci. Lett., 389, 23-33, doi:10.1016/j.epsl.2013.12.024, 2014.

Gale, A., Kennedy, W., Voigt, S., and Walaszczyk, I.: Stratigraphy of the Upper Cenomanian–Lower Turonian Chalk succession at Eastbourne, Sussex, UK: ammonites, inoceramid bivalves and stable carbon isotopes, Cretaceous Res., 26, 460-487, doi:10.1016/j.cretres.2005.01.006, 2005.

Gale, A., Voigt, S., Sageman, B., and Kennedy, W.: Eustatic sea-level record for the Cenomanian (Late Cretaceous)—extension to the Western Interior Basin, USA, Geology, 36, 859-862, doi:10.1130/G24838A.1, 2008.

Hilgen, F., Aziz, H. A., Krijgsman, W., Raffi, I., and Turco, E.: Integrated stratigraphy and astronomical tuning of the Serravallian and lower Tortonian at Monte dei Corvi (Middle–Upper Miocene, northern Italy), Palaeogeogr. Palaeocl., 199, 229-264, doi:10.1016/S0031-0182(03)00505-4, 2003.

Jarvis, I., Gale, A., Jenkyns, H., and Pearce, M.: Secular variation in Late Cretaceous carbon isotopes: a new $\delta^{13}C$ carbonate reference curve for the Cenomanian-Campanian (99.6-70.6 Ma), 143, 561-608, 2006.

Jenkyns, H. C., Gale, A. S., and Corfield, R. M.: Carbon- and oxygen-isotope stratigraphy of the English Chalk and Italian Scaglia and its palaeoclimatic significance, Geological Magazine, 131, 1-34, doi:10.1017/S0016756800010451, 1994.

Jenkyns, H. C., Matthews, A., Tsikos, H., and Erel, Y.: Nitrate reduction, sulfate reduction, and sedimentary iron isotope evolution during the Cenomanian-Turonian oceanic anoxic event, Paleoceanography, 22, PA3208, doi:10.1029/2006PA001355, 2007.

Kuiper, K., Deino, A., Hilgen, F., Krijgsman, W., Renne, P., and Wijbrans, J.: Synchronizing rock clocks of Earth history, Science, 320, 500-504, doi:10.1126/science.1154339, 2008.

Kuroda, J., Ogawa, N. O., Tanimizu, M., Coffin, M. F., Tokuyama, H., Kitazato, H., and Ohkouchi, N.: Contemporaneous massive subaerial volcanism and late cretaceous Oceanic Anoxic Event 2, Earth Planet Sc Lett, 256, 211-223, DOI 10.1016/j.epsl.2007.01.027, 2007.

Lanci, L., Muttoni, G., and Erba, E.: Astronomical tuning of the Cenomanian Scaglia Bianca Formation at Furlo, Italy, Earth Planet. Sci. Lett., 292, 231-237, doi:10.1016/j.epsl.2010.01.041, 2010.

Laskar, J., Fienga, A., Gastineau, M., and Manche, H.: La2010: a new orbital solution for the long-term motion of the Earth, Astron. Astrophys., 532, doi:10.1051/0004-6361/201116836, 2011a.

Laskar, J., Gastineau, M., Delisle, J., Farrés, A., and Fienga, A.: Strong chaos induced by close encounters with Ceres and Vesta., Astron. Astrophys., 532, 1-4, doi:10.1051/0004-6361/201117504 2011b.

Laurin, J., Meyers, S., Uličný, D., Jarvis, I., and Sageman, B.: Axial obliquity control on the greenhouse carbon budget through middle- to high-latitude reservoirs, 30, 133-149, 10.1002/2014PA002736, 2015.

Leckie, R. M.: Foraminifera of the Cenomanian-Turonian boundary interval, Greenhorn Formation, Rock Canyon Anticline, Pueblo, Colorado, in: Fine-grained deposits and biofacies of the Cretaceous Western Interior Seaway: Evidence of cyclic sedimentary processess: SEPM Field Trip Guidebook No. 4, edited by: Pratt, L., Kauffman, E., and Zelt, F., 139-155, 1985.

Ma, C., Meyers, S. R., Sageman, B. B., Singer, B. S., and Jicha, B. R.: Testing the astronomical time scale for oceanic anoxic event 2, and its extension into Cenomanian strata of the Western Interior Basin (USA), Geol. Soc. Am. Bull., doi:10.1130/b30922.1, 2014.

Meyers, S., and Sageman, B.: Quantification of deep-time orbital forcing by average spectral misfit, Am. J. Sci., 307, 773-792, doi:10.2475/05.2007.01, 2007.

Meyers, S., Sageman, B., and Arthur, M.: Obliquity forcing of organic matter accumulation during Oceanic Anoxic Event 2, Paleoceanography, 27, PA3212, doi:10.1029/2012PA002286, 2012a.

Meyers, S., Siewert, S., Singer, B., Sageman, B., Condon, D., Obradovich, J., Jicha, B., and Sawyer, D.: Intercalibration of radioisotopic and astrochronologic time scales for the Cenomanian-Turonian boundary interval, Western Interior Basin, USA, Geology, 40, 7-10, doi:10.1130/G32261.1, 2012b.

Meyers, S. R.: Seeing red in cyclic stratigraphy: Spectral noise estimation for astrochronology, Paleoceanography, 27, PA3228, doi:10.1029/2012PA002307, 2012.

Min, K., Mundil, R., Renne, P. R., and Ludwig, K. R.: A test for systematic errors in 40Ar/39Ar geochronology through comparison with U/Pb analysis of a 1.1-Ga rhyolite, Geochim. Cosmochim. Ac. , 64, 73-98, doi:10.1016/S0016-7037(99)00204-5, 2000.

Mitchell, R., Bice, D., Montanari, A., Cleaveland, L., Christianson, K., Coccioni, R., and Hinnov, L.: Oceanic anoxic cycles? Orbital prelude to the Bonarelli Level (OAE 2), Earth. Planet. Sc. Lett., 267, 1-16, doi:10.1016/j.epsl.2007.11.026, 2008.

Montanari, A., Chan, L., and Alvarez, W.: Synsedimentary Tectonics in the Late Cretaceous Early Tertiary Pelagic Basin of the Northern Apennines, Italy, in: Soc Econ Pa, edited by: Crevello, P. D., Wilson, J. L., Sarg, J. F., and Read, J. F., The Society of Economic Paleontologists and Mineralogists, 379-399, 1989.

Obradovich, J.: A Cretaceous time scale, in: Evolution of the Western Interior Basin, edited by: Caldzell, W. G. E., and Kauffman, E., Geological Association of Canada, 379-396, 1993.

Paillard, D., Labeyrie, L., and Yiou, P.: Macintosh program performs time-series analysis, Eos Trans. A. G. U., 77, 379, 1996.

Reimold, W. U., Koeberl, C., and Bishop, J.: Roter Kamm impact crater, Namibia: Geochemistry of basement rocks and breccias, Geochim. Cosmochim. Ac., 58, 2689-2710, doi:10.1016/0016-7037(94)90138-4, 1994.

Renne, P., Deino, A., Hilgen, F., Kuiper, K., Mark, D., Mitchell, W., Morgan, L., Mundil, R., and Smit, J.: Time Scales of Critical Events Around the Cretaceous-Paleogene Boundary, Science, 339, 684-687, doi:10.1126/science.1230492 2013.

Ruckstuhl, A. F., Jacobson, M. P., Field, R. W., and Dodd, J. A.: Baseline subtraction using robust local regression estimation, J. Quant. Spectrosc. Ra., 68, 179-193, doi:10.1016/S0022-4073(00)00021-2, 2001.

Sageman, B., Meyers, S., and Arthur, M.: Orbital time scale and new C-isotope record for Cenomanian-Turonian boundary stratotype, Geology, 34, 125-128, doi:10.1130/G22074.1, 2006.

Sageman, B. B., Singer, B. S., Meyers, S. R., Siewert, S. E., Walaszczyk, I., Condon, D. J., Jicha, B. R., Obradovich, J. D., and Sawyer, D. A.: Integrating 40Ar/39Ar, U-Pb, and astronomical clocks in the Cretaceous Niobrara Formation, Western Interior Basin, USA, Geol. Soc. Am. Bull., 126, 956-973, doi:10.1130/b30929.1, 2014.

Scopelliti, G., Bellanca, A., Neri, R., Baudin, F., and Coccioni, R.: Comparative high-resolution chemostratigraphy of the Bonarelli Level from the reference Bottaccione section (Umbria-Marche Apennines) and from an equivalent section in NW Sicily: Consistent and contrasting responses to the OAE2, Chem. Geol., 228, 266-285, doi:10.1016/j.chemgeo.2005.10.010, 2006.

Sinton, C., and Duncan, R.: Potential links between ocean plateau volcanism and global ocean anoxia at the Cenomanian-Turonian boundary, Econ. Geol. Bull. Soc., 92, 836-842, doi:10.2113/gsecongeo.92.7-8.836 1997.

Sissingh, W.: Biostratigraphy of Cretaceous calcareous nannoplankton, Geol. Mijnbouw, 56, 37-65, 1977.

Snow, L., Duncan, R., and Bralower, T.: Trace element abundances in the Rock Canyon Anticline, Pueblo, Colorado, marine sedimentary section and their relationship to Caribbean plateau construction and oxygen anoxic event 2, Paleoceanography, 20, PA3005, doi:10.1029/2004PA001093, 2005.

Sprovieri, M., Sabatino, N., Pelosi, N., Batenburg, S. J., Coccioni, R., Iavarone, M., and Mazzola, S.: Late Cretaceous orbitally-paced carbon isotope stratigraphy from the Bottaccione Gorge (Italy), Palaeogeogr. Palaeocl., 379–380, 81-94, doi:10.1016/j.palaeo.2013.04.006, 2013.

Stoll, H., and Schrag, D.: High-resolution stable isotope records from the Upper Cretaceous rocks of Italy and Spain: Glacial episodes in a greenhouse planet?, Geol. Soc. Am. Bull., 112, 308-319, doi:10.1130/0016-7606, 2000.

Stoll, H. M., and Schrag, D. P.: Sr/Ca variations in Cretaceous carbonates: relation to productivity and sea level changes, Palaeogeogr. Palaeocl., 168, 311-336, doi:10.1016/S0031-0182(01)00205-X, 2001.

Takashima, R., Nishi, H., Hayashi, K., Okada, H., Kawahata, H., Yamanaka, T., Fernando, A. G., and Mampuku, M.: Litho-, bio- and chemostratigraphy across the Cenomanian/Turonian boundary (OAE 2) in the Vocontian Basin of southeastern France, Palaeogeogr. Palaeocl., 273, 61-74, doi:10.1016/j.palaeo.2008.12.001, 2009.

Thomson, D. J.: Spectrum Estimation and Harmonic-Analysis, P. IEEE, 70, 1055-1096, doi:10.1109/PROC.1982.12433, 1982.

Trabucho-Alexandre, J., Tuenter, E., Henstra, G., van der Zwan, K., van de Wal, R., Dijkstra, H., and de Boer, P.: The mid-Cretaceous North Atlantic nutrient trap: Black shales and OAEs, Paleoceanography, 25, PA4201, doi:10.1029/2010pa001925, 2010.

Trabucho-Alexandre, J., Negri, A., and de Boer, P. L.: Early Turonian pelagic sedimentation at Moria (Umbria-Marche, Italy): Primary and diagenetic controls on lithological oscillations, Palaeogeogr. Palaeocl., 311, 200-214, doi:10.1016/j.palaeo.2011.08.021, 2011.

Tsikos, H., Jenkyns, H. C., Walsworth-Bell, B., Petrizzo, M. R., Forster, A., Kolonic, S., Erba, E., Silva, I. P., Baas, M., Wagner, T., and Damste, J. S. S.: Carbon-isotope stratigraphy recorded by the Cenomanian-Turonian Oceanic Anoxic Event: correlation and implications based on three key localities, J Geol Soc London, 161, 711-719, 2004.

Turgeon, S., and Creaser, R.: Cretaceous oceanic anoxic event 2 triggered by a massive magmatic episode, Nature, 454, 323-326, doi:10.1038/nature07076, 2008.

Voigt, S., Gale, A., and Voigt, T.: Sea-level change, carbon cycling and palaeoclimate during the Late Cenomanian of northwest Europe; an integrated palaeoenvironmental analysis, Cretaceous Res., 27, 836-858, doi:10.1016/j.cretres.2006.04.005, 2006.

Voigt, S., Erbacher, J., Mutterlose, J., Weiss, W., Westerhold, T., Wiese, F., Wilmsen, M., and Wonik, T.: The Cenomanian Turonian of the Wunstorf section (North Germany): global stratigraphic reference section and new orbital time scale for Oceanic Anoxic Event 2, Newsl Stratigr, 43, 65-89, doi:10.1127/0078-0421/2008/0043-0065, 2008.

Zachos, J. C., McCarren, H., Murphy, B., Röhl, U., and Westerhold, T.: Tempo and scale of late Paleocene and early Eocene carbon isotope cycles: Implications for the origin of hyperthermals, Earth Planet. Sc. Lett, 299, 242-249, doi:10.1016/j.epsl.2010.09.004, 2010.

Zheng, X.-Y., Jenkyns, H., Gale, A., Ward, D., and Henderson, G.: Changing ocean circulation and hydrothermal inputs during Ocean Anoxic Event 2 (Cenomanian–Turonian): evidence from Nd-isotopes in the European shelf sea, Earth Planet. Sc. Lett., 375, 338-348, doi:10.1016/j.epsl.2013.05.053, 2013.

Clim. Past Discuss., doi:10.5194/cp-2015-182, 2016
Manuscript under review for journal Clim. Past
Published: 26 January 2016

Climate of the Past Discussions
Open Access
EGU

7 Tables

Table 1. Astronomical tuning options for biostratigraphic and isotopic events and comparison to radioisotopic ages. Uncertainties on tuned absolute ages comprise the uncertainty in the stratigraphic position and/or correlation of an event (± 0.75 m) and the uncertainty in the astronomical target curve (Laskar et al., 2011a) (± 0.079 Myr). The numerical age of the C/T boundary is based on intercalibration of $^{40}Ar/^{39}Ar$ dating, U-Pb dating and astrochronology (Meyers et al., 2012b); Radioisotopic age of the Base of *Whiteinella archaeocretacea* is the weighted mean age of single and multicrystal $^{40}Ar/^{39}Ar$ ages of bentonite A; Radioisotopic ages for the first peak of the Mid-Cenomanian event come from single crystal $^{40}Ar/^{39}Ar$ dating of the Thatcher bentonite in the *Conlinceras tarrantense* zone (Calycoceras *gilberti*). All radioisotopic ages are reported in 2σ and using a FC age of 28.201 ± 0.46 ka (1σ)(Kuiper et al., 2008).

Event	**Stratigraphic Level (m)**	**Tuning #1 (Ma)** with stratigraphic and astronomical uncertainty	**Tuning #2 (Ma)** with stratigraphic and astronomical uncertainty	**Radioisotopic dating (Ma)** with 2σ radiometric uncertainty
***Hitch Wood* $\delta^{13}C$ excursion**	516.24 m	90.59 ± 0.15	90.99 ± 0.15	
Base D. primitiva - M. sigali	508.85 m	91.31 ± 0.15	91.72 ± 0.15	
***Round down* $\delta^{13}C$ excursion**	499.44 m	92.32 ± 0.15	92.72 ± 0.15	
Base NC14	493.85 m	92.93 ± 0.15	93.33 ± 0.15	
Base *Helvetoglobotruncana helvetica*	491.85 m	93.17 ± 0.15	93.57 ± 0.15	
C/T boundary	487.47 m	93.69 ± 0.15	94.10 ± 0.15	93.90 ± 0.15 (Meyers et al., 2012b)
Base *Whiteinella archaeocretacea*	485.70 m	94.17 ± 0.15	94.57 ± 0.15	94.20 ± 0.28 (Meyers et al., 2012b)
Base NC12	484.20 m	94.28 ± 0.15	94.68 ± 0.15	
Base CC10	482.77 m	94.39 ± 0.15	94.79 ± 0.15	
first peak Mid-Cenomanian event	466.47 m	96.09 ± 0.15	96.49 ± 0.15	96.21 ± 0.36 this study

Clim. Past Discuss., doi:10.5194/cp-2015-182, 2016
Manuscript under review for journal Clim. Past
Published: 26 January 2016

Climate of the Past Discussions
Open Access
EGU

8 Figures

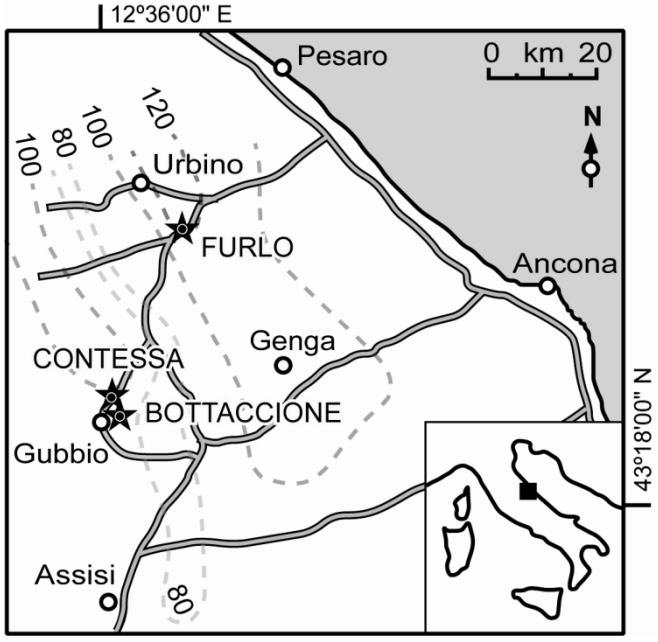

Figure 1. Geographic setting of the study sections with isopachs of the Bonarelli level (in cm) from Montanari et al.(1989).

Clim. Past Discuss., doi:10.5194/cp-2015-182, 2016
Manuscript under review for journal Clim. Past
Published: 26 January 2016

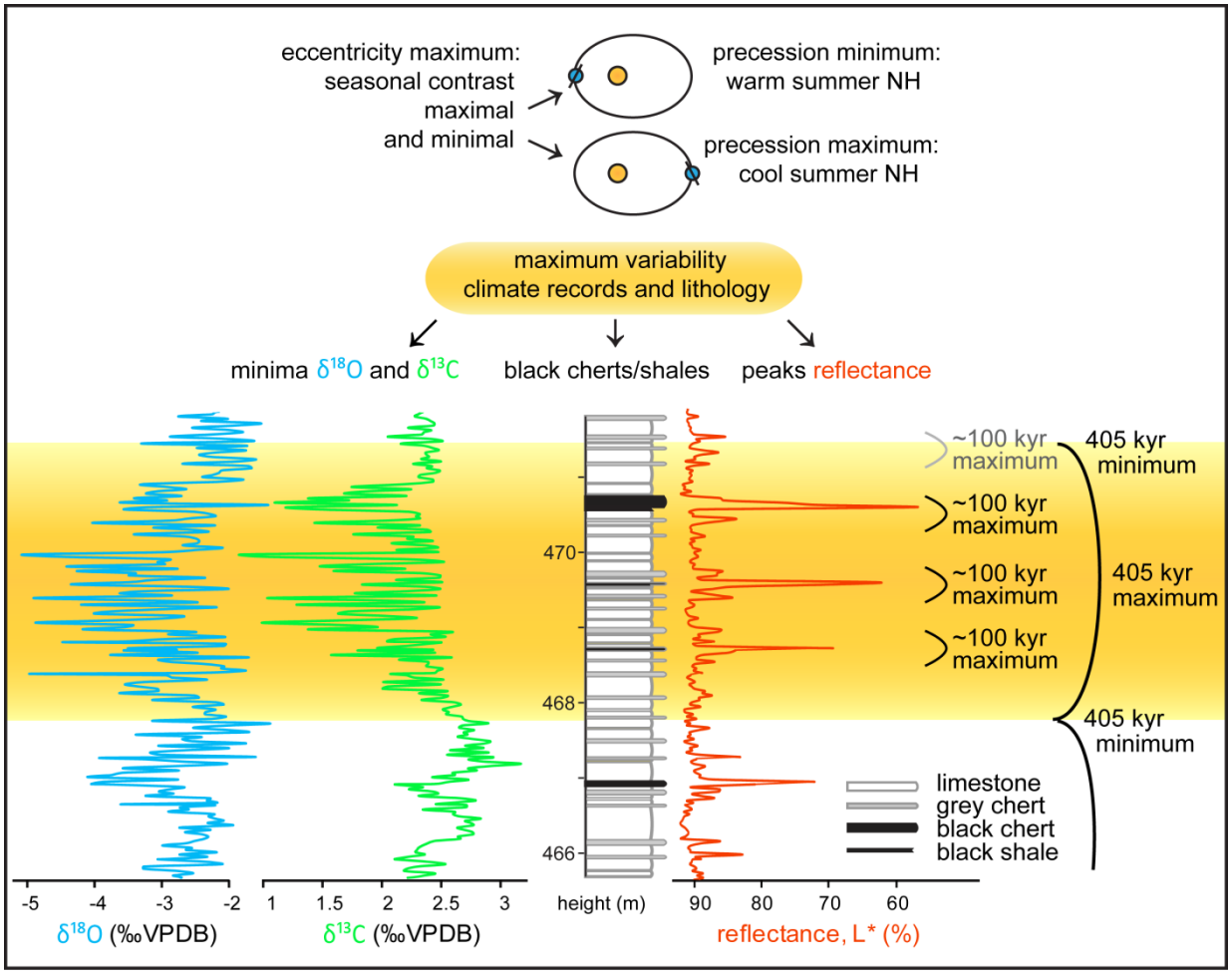

Figure 2. Phase relationship between eccentricity and proxy records. During eccentricity maxima, the seasonal contrast for the NH is maximally enhanced during precession minima and maximally reduced during precession maxima (top: schematic representation of the Earth's orbit around the sun). Hence, climate variability is strongly amplified during eccentricity maxima, triggering the highest variability in the climate-sensitive records and hierarchical organization of chert-limestone alternations.

Clim. Past Discuss., doi:10.5194/cp-2015-182, 2016
Manuscript under review for journal Clim. Past
Published: 26 January 2016

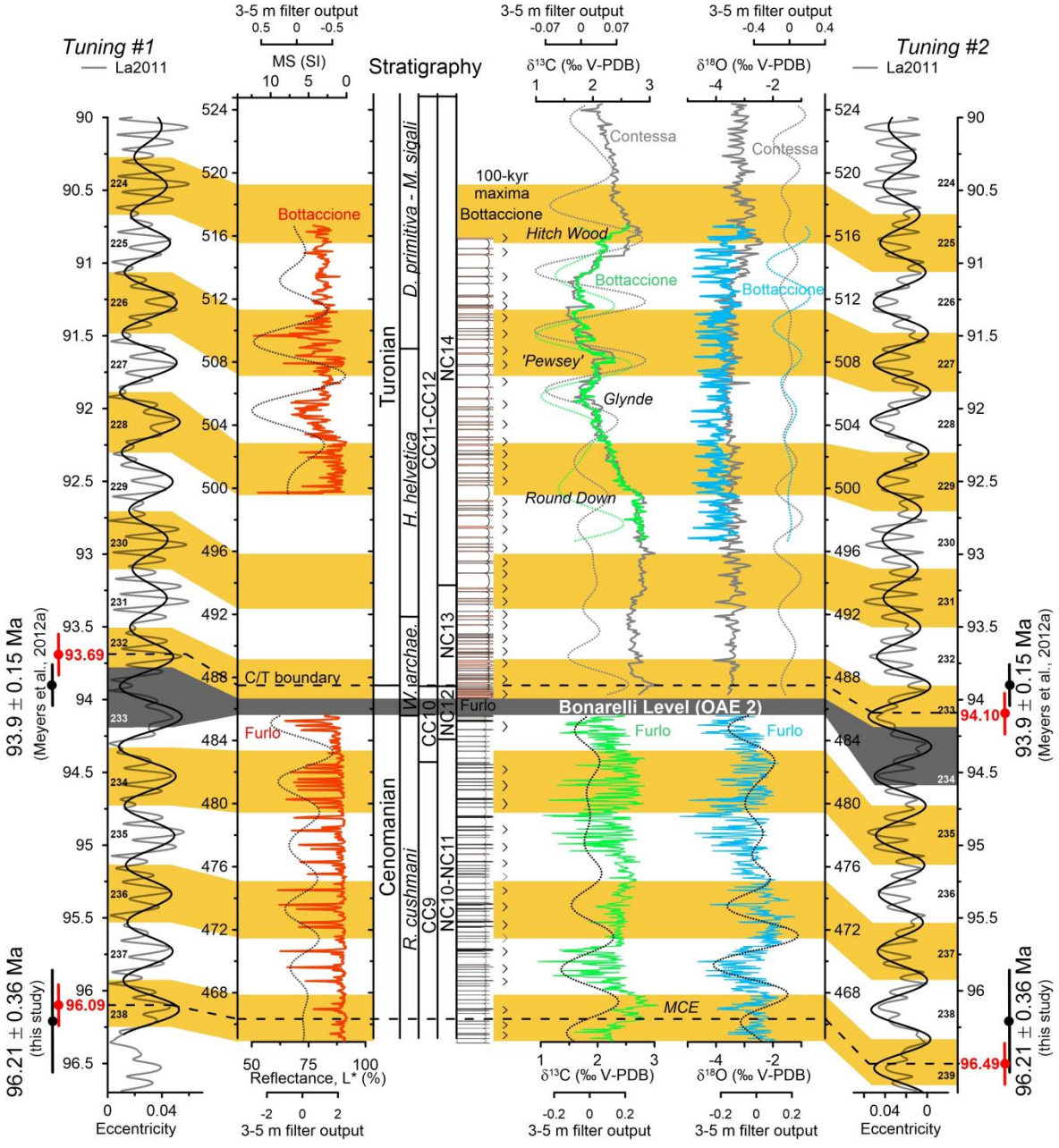

Figure 3. Cyclostratigraphic interpretation of the C/T interval of the Umbria-Marche basin. Circumflexes indicate 100-kyr bundles of precession-paced lithological alternations, further grouping in 405-kyr cycles is indicated by alternating yellow-white bands. Geophysical records (L* and MS) accentuate the hierarchical stacking pattern. Stable isotope ratios show increased amplitude and a tendency towards more negative values during eccentricity maxima. Isotopic records in grey are

Clim. Past Discuss., doi:10.5194/cp-2015-182, 2016
Manuscript under review for journal Clim. Past
Published: 26 January 2016

Climate of the Past Discussions
Open Access
EGU

from Stoll and Schrag (2000). Event names in italics refer to nomenclature of Jarvis et al. (2006). Astronomical tuning options to La2011 are presented, with 405-kyr cycle numbering back from the present day, next to radioisotopic ages discussed in this study.

Clim. Past Discuss., doi:10.5194/cp-2015-182, 2016
Manuscript under review for journal Clim. Past
Published: 26 January 2016

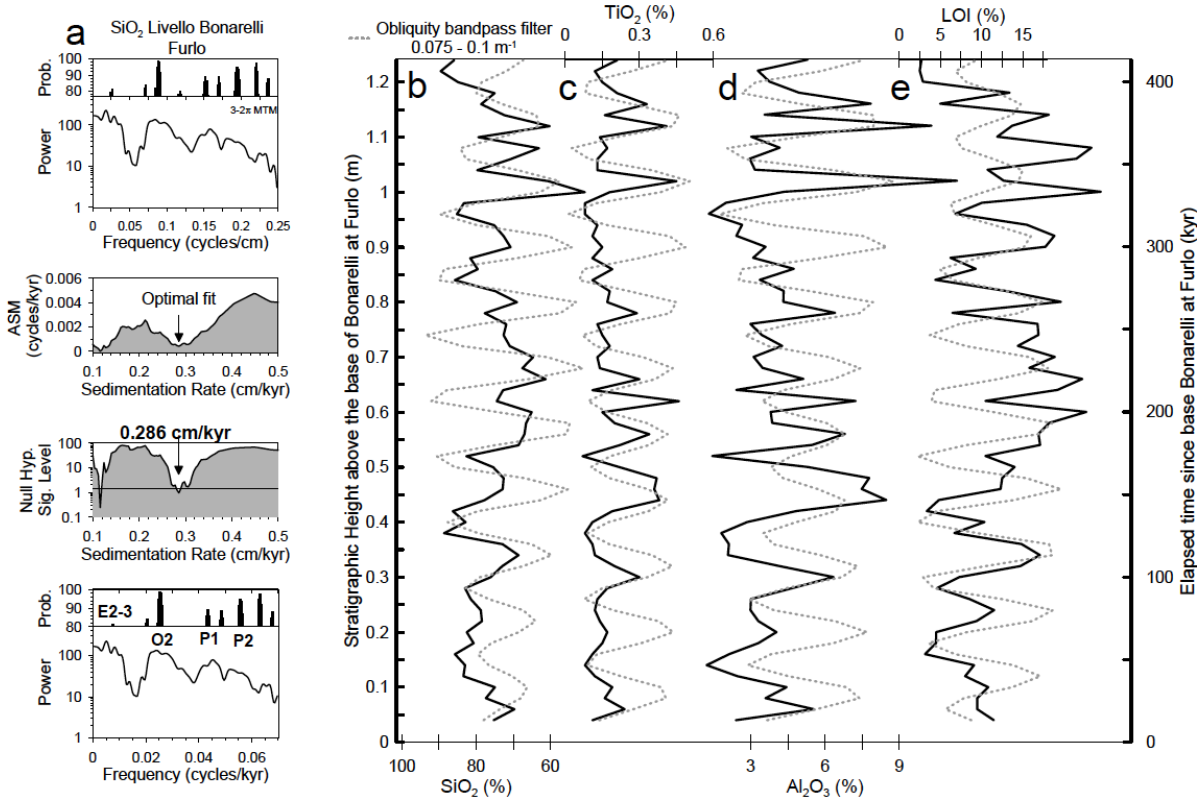

Figure 4. Duration estimate of Livello Bonarelli at Furlo based on **(a)** the Average Spectral Misfit (ASM) method. **(b-e)** SiO_2, TiO_2, and Al_2O_3 contents and Loss on Ignition (LOI) data show ~12-cm-thick cycles, interpreted as obliquity. The duration of Livello Bonarelli at Furlo is estimated at 413 kyr.

Clim. Past Discuss., doi:10.5194/cp-2015-182, 2016
Manuscript under review for journal Clim. Past
Published: 26 January 2016

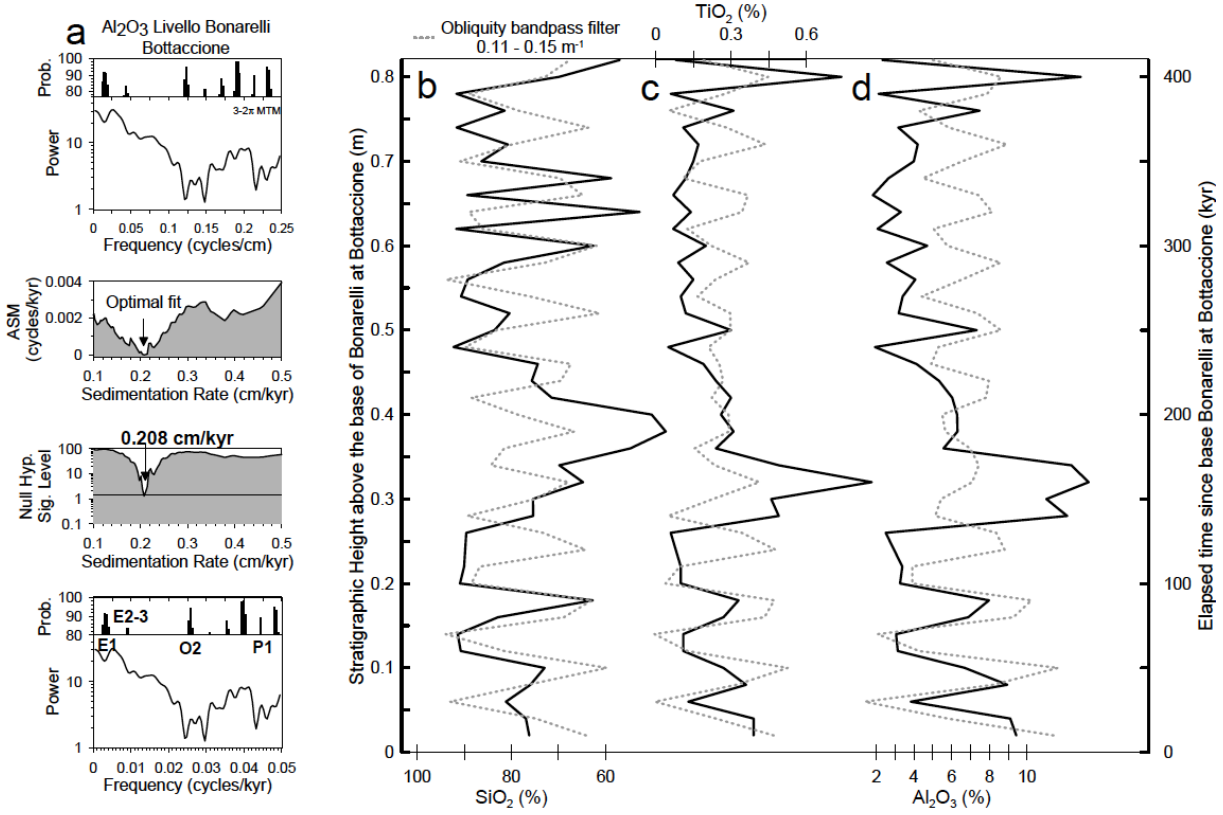

Figure 5. Duration estimate of Livello Bonarelli at Bottaccione based on (a) the Average Spectral Misfit (ASM) method. (b-d) SiO_2, TiO_2 and Al_2O_3 data show ~8-cm thick cycles, interpreted as obliquity. The duration of Livello Bonarelli at Bottaccione is estimated at 410 kyr.

Clim. Past Discuss., doi:10.5194/cp-2015-182, 2016
Manuscript under review for journal Clim. Past
Published: 26 January 2016

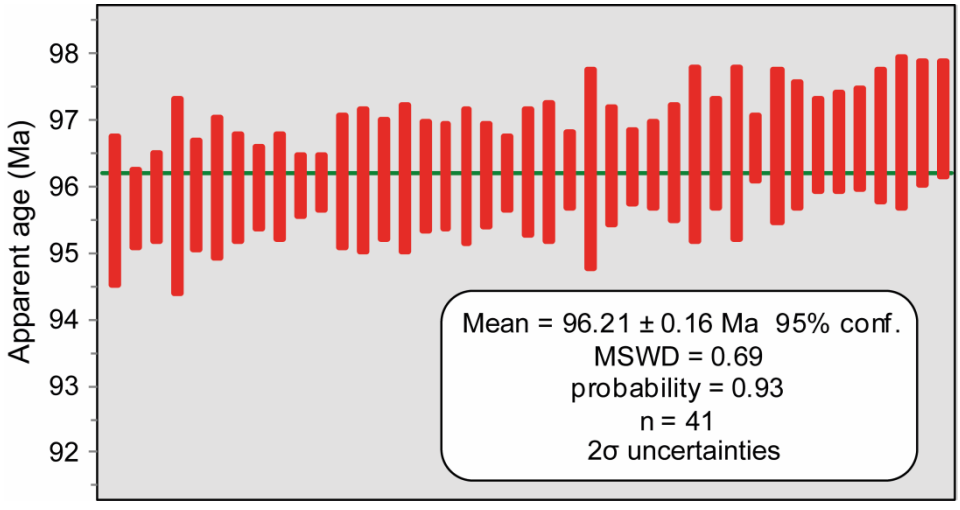

Figure 6. Summary of $^{40}Ar/^{39}Ar$ results

Clim. Past Discuss., doi:10.5194/cp-2015-182, 2016
Manuscript under review for journal Clim. Past
Published: 26 January 2016

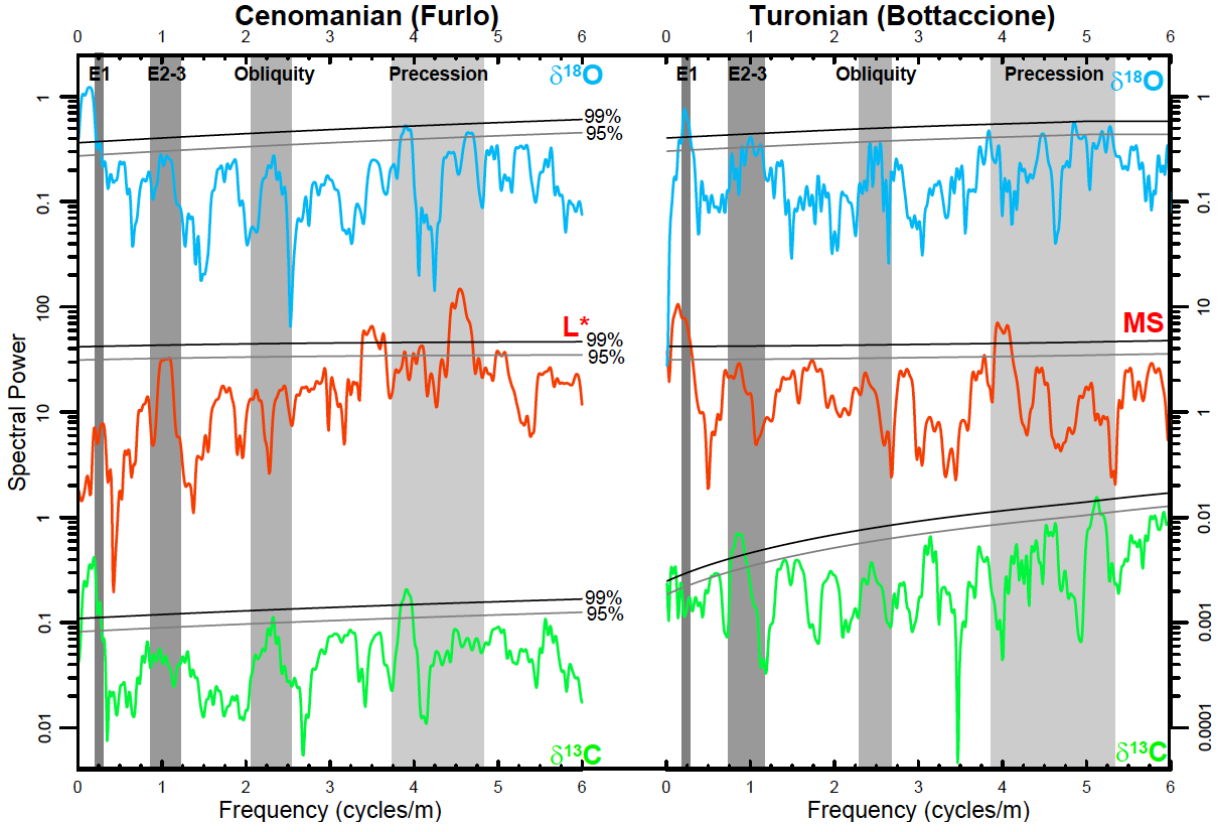

Figure 7. MTM/LOWSPEC spectra of proxy records. All proxy records show a strong imprint of eccentricity-modulated precession (E2-3: short eccentricity), $\delta^{13}C$ from Furlo also displays a statistically significant (>95% confidence level) imprint of obliquity.

Clim. Past Discuss., doi:10.5194/cp-2015-182, 2016
Manuscript under review for journal Clim. Past
Published: 26 January 2016

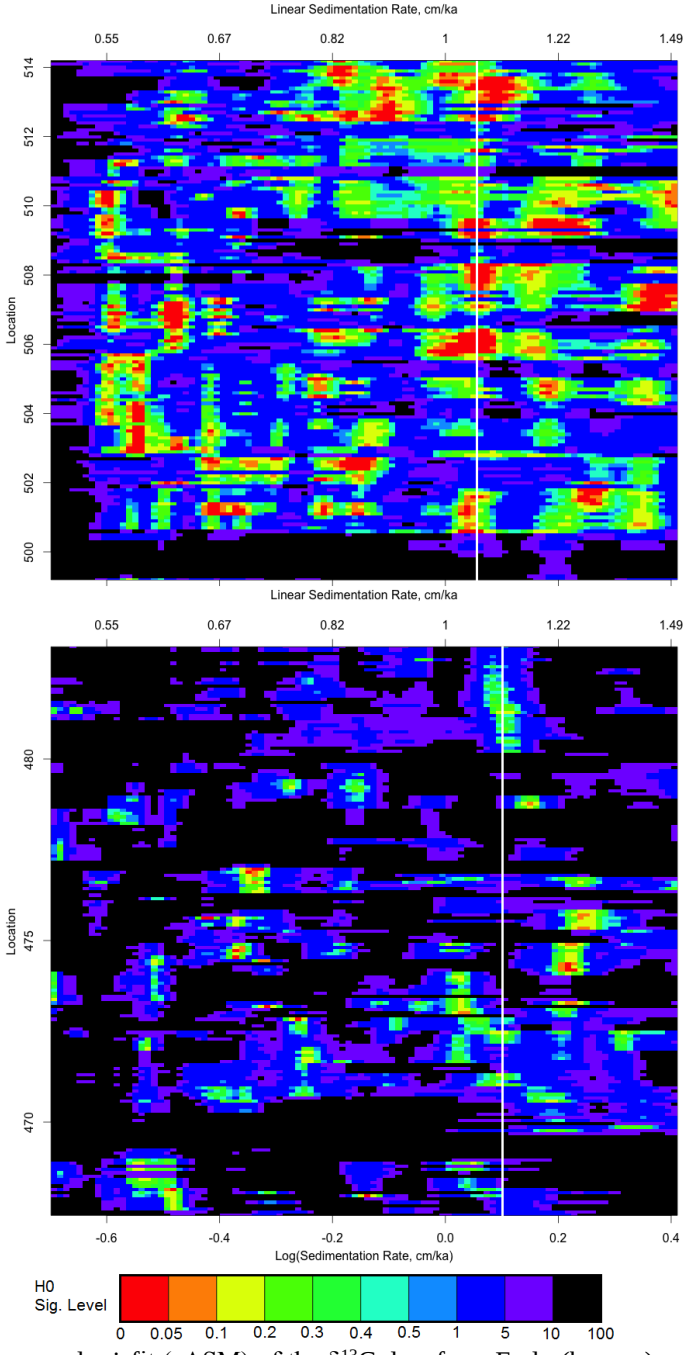

Figure 8. Evolutionary average spectral misfit (eASM) of the $\delta^{13}C$ data from Furlo (bottom) and Bottaccione (top), with a 5 m window, 0.1 m steps and using those frequencies with F-test > 80%. The white line suggests a stable sedimentation rate of 1.1 cm/kyr in Furlo and 1.05 cm/kyr in Bottaccione.

Clim. Past Discuss., doi:10.5194/cp-2015-182, 2016
Manuscript under review for journal Clim. Past
Published: 26 January 2016

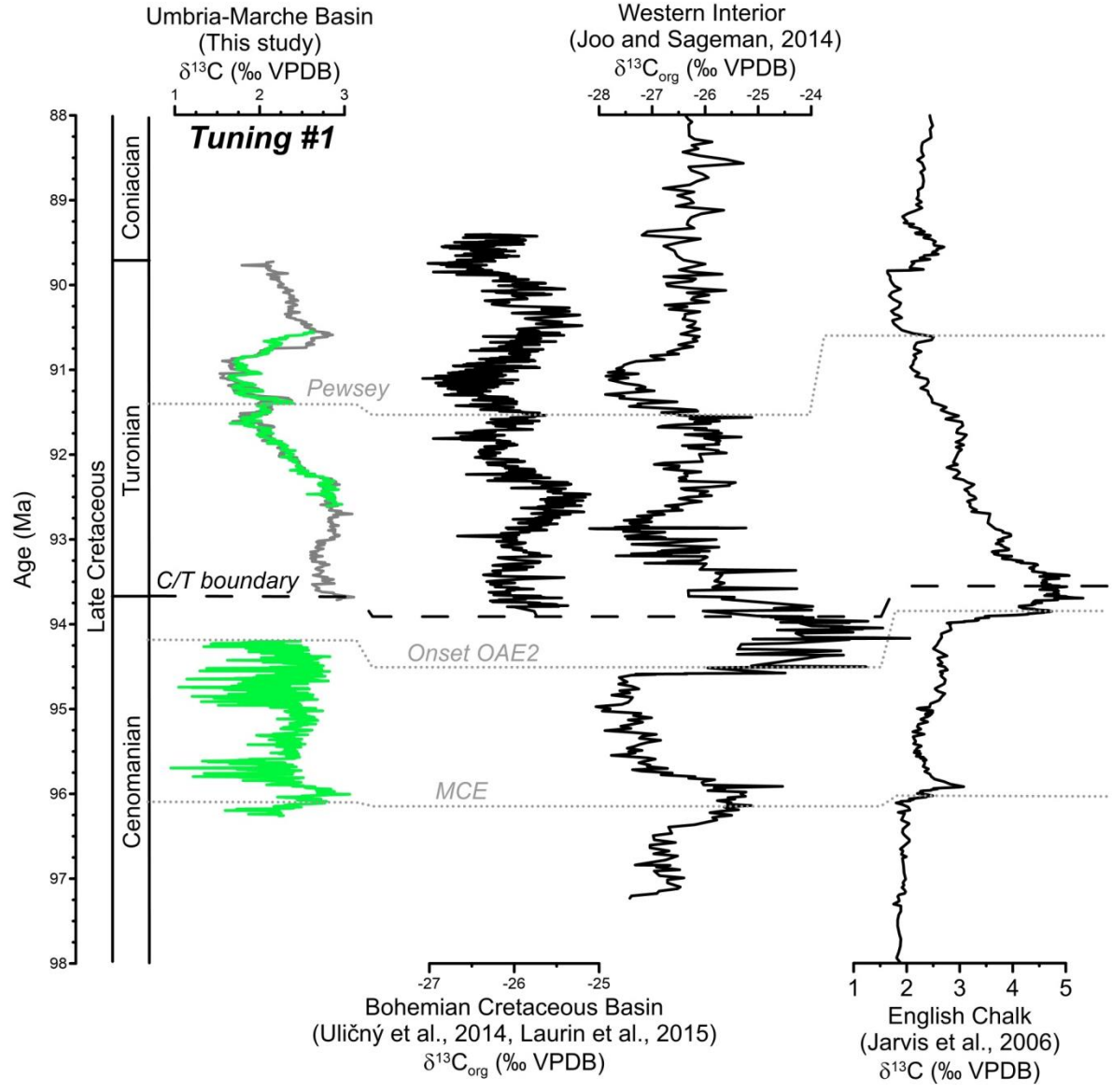

Figure 9. Global correlation of $\delta^{13}C_{carb}$ data of the Cenomanian-Turonian interval.